树脂基复合材料用陶瓷涂层防护性能分析

郭面焕, 刘爱国, 高嘉爽, 赵敏海*
(哈尔滨工业大学 现代焊接生产技术国家重点实验室, 哈尔滨 150001)

摘 要: 采用等离子喷涂铝粉作为打底材料在碳纤维增强聚酰亚胺复合材料(PMC)基体上制备了 Al_2O_3 和 ZrO_2 轻质陶瓷防护涂层, 测试了涂层的剪切结合强度、耐热循环性能、抗冲蚀性能、隔热性能。结果表明, 等离子喷涂铝粉作打底层的涂层系统, 性能优于电弧喷铝或电弧喷锌作打底层的涂层系统。带有 Al_2O_3 涂层的试样失重不到基体材料失重的 1/3 Al_2O_3 和 ZrO_2 陶瓷涂层都可以为聚酰亚胺复合材料基体提供有效的冲蚀防护。Al_2O_3 和 ZrO_2 陶瓷涂层都可以为聚酰亚胺复合材料基体提供有效的隔热防护, ZrO_2 涂层隔热性能优于 Al_2O_3 涂层。

关键词: 高温树脂基复合材料; 陶瓷涂层; 冲蚀; 隔热涂层
中图分类号: TG148 文献标识码: A 文章编号: 0253-360X(2005)11-13-04

郭面焕

0 序 言

高温树脂基复合材料出现以来, 由于其工作温度高, 高温性能优异, 比强度、比刚度高, 已广泛应用于航空航天领域。美国在 20世纪 80年代初期就已将聚酰亚胺基高温复合材料用于战斗机发动机的制造, 到现在该技术已日臻成熟并发展了系列产品[1]。为提高树脂基复合材料的耐高温性能和耐冲蚀性能, 各国研究工作者进行了广泛的研究。碳纤维/聚酰亚胺的耐热温度是 300 ℃左右, 但在其外表面加上氧化硅涂层, 可使其在 400 ℃甚至更高的温度下使用[2], 铝涂层的应用可以使碳纤维/聚酰亚胺的抗高温氧化能力增加[3]。为了找到适合于发动机上高温树脂基复合材料上应用的耐高温抗冲蚀涂层, NASA Glenn Research Center和 Allison Advanced Development Company合作, 在碳纤维增强聚酰亚胺树脂基复合材料 T650-35/PMR-15上试验了采用两种底层材料和三种耐磨性良好的顶层材料的不同涂层系统, 其中顶层材料分别为 Cr_3C_2-NiCr, WC-Co, TN, 在随后的热循环响应和耐冲蚀磨损性能试验中发现, Cr_3C_2-NiCr及 WC-Co涂层材料表现出良好的耐冲蚀性能, 是未防护的聚酰亚胺树脂基复合材料的 8.5倍[4,5], 采用等离子喷涂获得的涂层性能远高于采用 CVD(化学气相乘积)方法获得的 TN涂层[6]。采用电弧喷锌作为打底层, 等离子喷涂 Al_2O_3 作为防护涂层, 在高温树脂基复合材料上制备出了轻质陶瓷防护涂层[7], 涂层和基体结合强度高, 抗热震性能好。为了进一步提高防护涂层和基体的结合强度及耐热循环性能, 采用等离子喷涂铝粉作为打底层, 制备了高温树脂基复合材料轻质防护涂层, 研究了防护陶瓷涂层的隔热和耐冲蚀性能。

1 试验材料及方法

试验的基体材料为某航空研究单位开发的碳纤维增强聚酰亚胺复合材料, 该材料可在 371 ℃下长期稳定工作, 瞬时耐温可达 500 ℃。防护涂层采用了两种材料, 一种是加有 13% TiO_2 的 Al_2O_3 粉末, 另一种是 Y_2O_3 部分稳定的 ZrO_2。这两种陶瓷涂层都采用等离子喷涂方法制备。打底材料为等离子喷涂纯铝粉。聚酰亚胺复合材料平板在喷涂前经过喷砂粗化处理。所用等离子喷涂设备为瑞士 PT公司生产的 R-750C等离子喷涂设备, 喷涂工艺参数见表 1。

涂层与基体的结合强度参照国标 GB/T 7124-1986《胶粘剂拉伸剪切强度测定方法》测定, 试样为宽 20 mm、长 40 mm、厚 2 mm 平板。将喷涂好的试样涂层一侧用强力胶粘贴在预先喷砂处理过的 2mm厚钢板上, 制成拉伸试样。粘贴部分宽度 15 mm左右。待粘贴好的试样经 24 h室温固化后,

收稿日期: 2005-09-12
基金项目: 国家 863计划项目(2002AA331080)
*参加此项研究工作的还有马 宏, 胡海龙

表 1 防护涂层等离子喷涂工艺参数

Table 1 Process parameters of plasma spraying for thermal and erosion-resistant coatings

涂层	喷涂电流 I/A	喷涂电压 U/V	喷涂距离 l/mm
铝打底层	400	40	140
Al_2O_3涂层	550	40	100
ZrO_2涂层	580	40	100

在 Instron 1186电子万能材料试验机上拉伸，直至涂层脱落。记录最大拉伸力，测量涂层开裂面积，计算出涂层剪切结合强度。采用 OLYMPUS PMG3显微镜对涂层进行金相组织观察。

热循环试验采用加热、保温、浸入室温的水中进行冷却的方式循环进行。将喷涂好的试样在电炉中加热到 371 ℃，保温 10 min，取出浸入室温的水中，用放大镜观察冷却后的试样表面，记录第一次发现裂纹时的浸水冷却次数，定为启裂次数。为了和前期试验结果进行对比，在进行浸水冷却循环试验前，先进行了 50个加热、保温、空冷循环。

冲蚀试验采用自制的冲蚀试验机进行。试样固定装置的角度可以调节，喷枪到试样的距离也可以根据需要进行调节。设备还备有用于观察的玻璃窗和清理残砂的通道。表 2为冲蚀试验各项参数值。冲蚀采用每次给砂量确定的方法，每次冲蚀用砂 0.25 kg，每次冲蚀完毕之后进行试样称重，称重采用精度为万分之一的天平。采用 S-5700型扫描电镜对冲蚀试样表面形貌进行观察。

表 2 冲蚀工艺参数

Table 2 Process parameters of erosion test

项目	砂粒类型	粒度 d/mm	冲蚀压力 p/MPa	冲蚀距离 l/mm
参数	棕刚玉	0.5	0.3	100

隔热试验是将试件有涂层的一面面对 300 ℃热源固定，采用红外线测温仪测量另一侧复合材料的温度。每隔 5 s测量一次。

2 结果与讨论

2.1 等离子喷涂铝粉作为打底层

前期研究结果表明[7]，电弧喷铝作为聚酰亚胺基复合材料防护涂层的打底层，会对基体产生烧损，涂层和基体的结合强度只有 7.54 MPa，采用电弧喷锌作为打底材料，涂层结合强度为 10.45 MPa。为进一步提高防护涂层和基体的结合强度及耐热循环能力，尝试了采用等离子喷铝作为打底层，在其上喷涂 Al_2O_3涂层及 ZrO_2涂层作为冲蚀防护及隔热涂层。Al/Al_2O_3涂层显微组织见图 1。

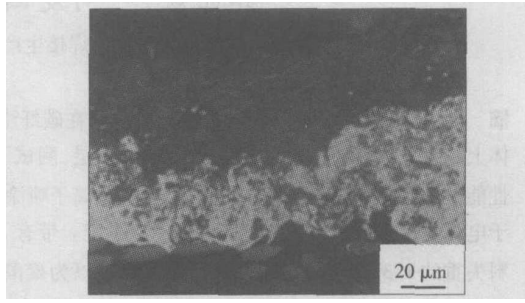

图 1 等离子喷铝打底层+Al_2O_3涂层微观形貌

Fig. 1 Microstructure of Al_2O_3 coating with Al as bond coating

由图 1可以看出，和电弧喷涂的铝打底层不同，等离子喷涂的铝打底层和基体结合良好，界面处没有烧损带的存在。

电弧喷涂采用的材料是铝丝材，丝材端部必须被加热到铝的熔点以上一段时间，才能形成液滴，在压缩空气的作用下被雾化，喷涂到基材上。铝丝材在电弧中加热时间长、过热度大，给基体带去的热量多，造成基体温升过高，使界面处基体烧损。尽管等离子弧的温度比电弧要高，但等离子喷涂时使用的材料是铝粉末，粉末进入等离子弧后立刻被喷涂到基体上，加热时间很短，铝粉的过热度较小，没有造成基体的烧损。剪切结合强度测试结果和前期试验结果对比见表 3。可以看出，等离子喷涂铝打底层和基体的结合强度为 11.89 MPa，不仅高于电弧喷铝作打底层的涂层系统，而且也高于电弧喷锌作打底层的涂层系统。热循环试验结果和前期试验结果对比见表 4。

表 3 不同打底层的剪切试验结果

Table 3 Shear test results of different bond coating

打底层材料	开裂部位	剪切结合强度 τ/MPa
电弧喷涂锌	打底层开裂	10.45
电弧喷涂铝	基体开裂	7.54
等离子喷涂铝	打底层开裂	11.89

聚酰亚胺复合材料的工作温度较高，通常在 300 ℃以上。锌作为打底层材料，虽然和基体结合良好，塑性也很好，但在这样高的温度下，其本身强

表 4　涂层热循环试验数据

Table 4　Thermal cycling data of different coating

打底层	工作陶瓷层	启裂次数
电弧喷涂锌	Al_2O_3	31
电弧喷涂铝	Al_2O_3	23
等离子喷涂铝	ZrO_2	34
等离子喷涂铝	Al_2O_3	37

度降低较严重,降低了涂层系统的耐热循环能力,涂层在第 31个循环即发生了开裂。铝的熔点远高于锌的熔点,当聚酰亚胺复合材料在较高温度下工作时,其本身强度比锌打底层高,同样加热冷却情况下,等离子喷铝作为打底层的涂层系统分别在第 34个和第 37个循环时才产生裂纹。电弧喷铝作打底层的涂层系统在第 23个循环发生了开裂,是由于基体发生了烧损造成的。

2.2　防护涂层的耐冲蚀性能

图 2为冲蚀试验后,不带防护涂层和带有陶瓷防护涂层的试样的表面形貌。冲蚀攻角为 30°。

可以看出,没有防护涂层的聚酰亚胺复合材料表面冲蚀破坏严重,表层的聚酰亚胺和增强碳纤维已被冲蚀掉,基体内部碳纤维暴露出来。冲蚀造成了大量碳纤维断裂,见图 2a。碳纤维断裂将极大地影响复合材料的强度,而且碳纤维暴露在空气中,在较高温度下,容易发生氧化反应,给复合材料带来进一步的损伤。而带有陶瓷防护涂层的试样冲蚀后,仅发生了表面陶瓷涂层的轻微冲蚀,完全没有伤及基体材料,见图 2b、图 2c。

图 3为聚酰亚胺复合材料基体及带有陶瓷涂层试样的冲蚀失重曲线,冲蚀攻角为 30°。可以看出,在同样冲蚀条件下,带有 Al_2O_3 涂层的试样失重不到基体失重的 1/3,带有 ZrO_2 涂层的试样失重约为基体失重的 1/2。而且,Al_2O_3 涂层的密度约为基体材料密度的 2倍,ZrO_2 涂层的密度约为基体材料密度的 4倍,考虑其体积损失,陶瓷涂层的冲蚀磨损量仅为聚酰亚胺复合材料基体的 1/8左右。陶瓷涂层对聚酰亚胺复合材料起到了很好的保护作用。

图 4是带有 Al_2O_3 防护涂层的试样在不同冲蚀攻角下冲蚀失重的比较。可以看出,冲蚀攻角为 90°时涂层质量损失严重,冲蚀用砂量 0.5 g时,涂层失重已超过 20 g;小攻角冲蚀时涂层的耐冲蚀性较好,冲蚀用砂量 1.25 g时,涂层失重不到 10 g,表现出典型的脆性材料冲蚀特征。

2.3　防护涂层的隔热性能

图 5为涂层隔热性能的测试结果。可以看出,

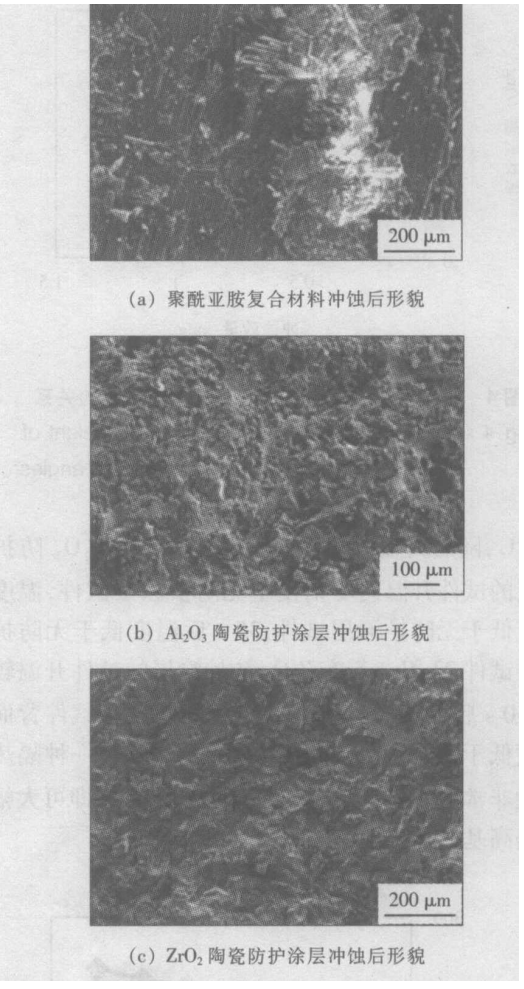

图 2　试样冲蚀后微观形貌

Fig. 2　Microstructures of samples after erosion

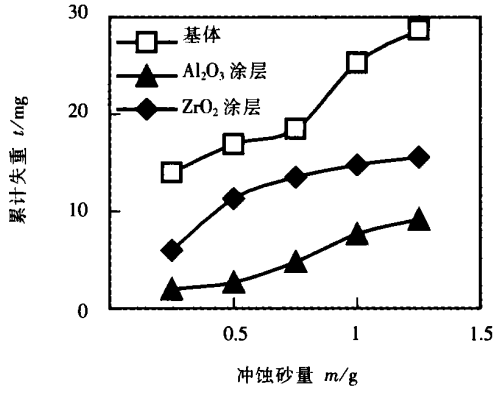

图 3　冲蚀失重和冲蚀砂量的关系

Fig. 3　Relationship of erosion losses and weight of erosion particles

Al_2O_3 和 ZrO_2 两种涂层都有较好的隔热作用。没有防护涂层的基体材料升温较快,10 s后即达到

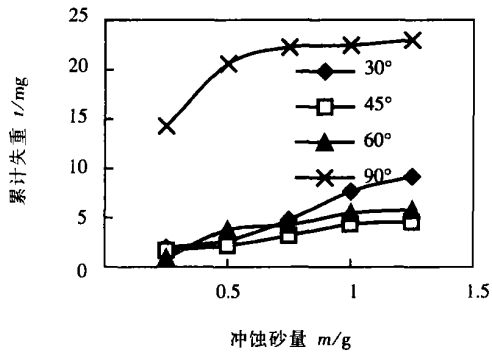

图 4 不同冲蚀攻角下冲蚀失重和冲蚀砂量的关系

Fig. 4 Relationship of erosion losses and weight of erosion particles with different impact angles

198 ℃, 随后升温速度逐渐减缓。带有 Al_2O_3 防护涂层的试件升温速度稍慢于无防护涂层试件, 温度一直低于无防护涂层试件, 35 s后温度低于无防护涂层试件 23 ℃。带有 ZrO_2 防护涂层的试件升温较慢, 10 s后, 试样背面仅为 59 ℃。35 s后, 试件背面温度低于无防护涂层试件 41 ℃。ZrO_2 是一种隔热性能非常好的陶瓷材料, 采用很薄的涂层, 即可大幅度提高基体材料的使用温度。

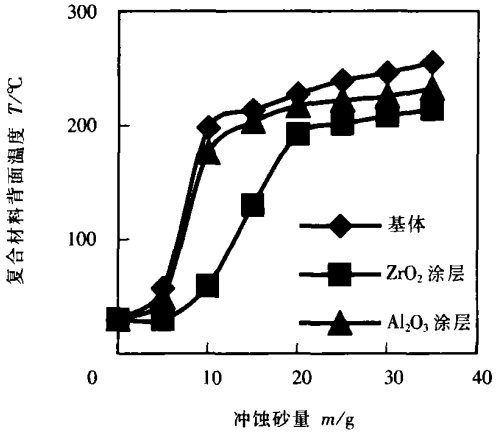

图 5 陶瓷防护涂层的隔热性能

Fig. 5 Thermal resistance of ceramic coating

3 结 论

(1) 在聚酰亚胺复合材料上采用等离子喷涂铝粉作打底涂层, 可以获得比电弧喷铝或电弧喷锌作打底层更高的结合强度, 是一种更好的打底涂层。采用等离子喷铝在聚酰亚胺复合材料上制备的 Al_2O_3 和 ZrO_2 陶瓷涂层的抗热震性能都优于电弧喷铝或电弧喷锌作打底层的涂层系统。

(2) 在同样冲蚀条件下, 带有 Al_2O_3 涂层的试样失重不到基体失重的 1/3, 带有 ZrO_2 涂层的试样失重约为基体失重的 1/2。Al_2O_3 和 ZrO_2 陶瓷涂层都可以为聚酰亚胺复合材料基体提供有效的冲蚀防护。在高攻角冲蚀条件下, 陶瓷涂层冲蚀较严重, 小攻角冲蚀条件下, 陶瓷涂层冲蚀轻微, 表现出典型的脆性材料冲蚀特征。

(3) Al_2O_3 和 ZrO_2 陶瓷涂层都可以为聚酰亚胺复合材料基体提供有效的隔热防护, ZrO_2 陶瓷涂层隔热性能优于 Al_2O_3 涂层。

参考文献:

[1] 谭必恩, 益小苏. 航空发动机用 PMR聚酰亚胺树脂基复合材料[J]. 航空材料学报, 2001, 21(1): 55-62

[2] 贾志刚. 树脂基复合材料隔热涂层的研究进展[J]. 材料保护, 2002, 35(2): 7-8

[3] Frances I Hurwitz. Effect of a coating on the thermo oxidative stability of celion 6000 graphite fiber/PMR 15 polyimide composites[J]. Composites Technology Review, 1983, 5(4): 109-114

[4] Meador M A, Sutter J K, Leissler G, *et al*. Coatings for high temperature polymer composites[A]. International SAMPE Symposium and Exhibition[C], 2001.

[5] Naik Subhash K, Macri Francis G, Dennis K, *et al*. Erosion coatings for high temperature polymer composites[A]. International SAMPE Symposium and Exhibition[C], 1999.

[6] Knight R, Ivosevic M, Twardowski K S, *et al*. Development of HVOF sprayed erosion/oxidation resistant coatings for composite structural components in propulsion systems[A]. Proceedings of USAF High Temple Workshop XXII[C], 2002.

[7] Zhang Yanliang, Guo Mianhuan, Liu Aiguo, *et al*. Depositing light ceramic coating on high temperature polymer matrix composite substrate[J]. Transactions of the China Welding Institution, 2005, 26(3): 5-8.
张艳良, 郭面焕, 刘爱国, 等. 高温树脂基复合材料防护用轻质陶瓷涂层的制备[J]. 焊接学报, 2005, 26(3): 5-8

作者简介: 郭面焕, 男, 1952年 7月出生, 高级工程师。主要从事各种金属材料焊接性的研究、焊接材料的研制、热喷涂表面改性的研究等方面的工作。发表论文 50余篇, 获省部级奖 2项, 发明专利 5项。

Email: guomianhuan@sohu.com

MAIN TOPICS, ABSTRACTS & KEY WORDS

Characteristic and recognition of ultrasonic TOFD signal and image for planar defect CHI Da-zhao, GANG Tie, YUAN Yuan, LV Pin (State Key Lab of Advanced Welding Production Technology, Harbin Institute of Technology, Harbin 150001, China). p1 - 4

Abstract: Considering several typical planar defects that were common flaws in thick aluminum weld, the characteristics of Ultrasonic TOFD (time of flight diffraction) was studied. Ultrasonic TOFD A-scan signal and B, D-scan image were analyzed and interpreted. Linearization was introduced in processing B and D-scan image. The results show that planar defect can be effectively recognized, located and sized by the characteristics of the received signal and image. Linearization effectively improves time resolution of the received images, which makes the characteristics of the defect more markedly and leads to more accurate quantitative measurement.

Key words: ultrasonic TOFD; characteristic and recognition; planar defect; linearization

Joining of TiAl intermetallic by self-propagating high-temperature synthesis CAO Jian, FENG Ji-cai, LI Zhuo-ran (State Key Lab of Advanced Welding Production Technology, Harbin Institute of Technology, Harbin 150001, China). p5 - 7

Abstract: A novel approach for joining TiAl by self-propagating high-temperature synthesis (SHS) was studied in the study. The Ti, Al and C powders with large exothermic enthalpy and the assisted electromagnetic field were applied in the joining processing. The typical joint was composed of three reaction zones. Adjacent to the TiAl base metal, a dark $TiAl_3$ reaction layer was observed on the interface. The TiC particles and Ti-Al compounds were found in the interlayer. It was also noted that in every condition the porosity could not be avoid due to the differences in specific volume between products and reactants, the evaporation of impurities, and the expansion of the gas trapped in the porosity of the reactant compact. In order to solve these problem, Ag-Cu brazing foils were placed between the powder compacts and the TiAl substrate. It was considered that molten Ag-Cu in the filler during SHS reaction improved the wettability of interlayer to TiAl substrate and filled well into the holes in the reaction products of the interlayer. In this way, the density could be increased and the joint quality could be improved.

Key words: TiAl alloys; self-propagating high-temperature synthesis (SHS); joining; microstructure

Study of the BCTW's phenomenon and characteristics in EBW ZHOU Qi[1], LIU Fang-jun[2], GUAN Qiao[2] (1. Ningbo Sub-academy of the National Weapons Science Research Academy, Ningbo 315103, Zhejiang, China; 2. Beijing Aeronautical Manufacturing Technology Research Institute, Beijing 100024, China; 3. Beijing University of Aeronautics & Astronautics, Beijing 100083, China). p8 - 12

Abstract: Two physical processes of the energy conversion and the current conduction were analyzed in the dynamic process of EBW. According to the characteristics of EBW process, the beam current through workpiece during EBW process was studied using the special multichannel device to collect current signal. The characteristics of the time domain, frequency domain, sequencing, conducting ratio of BCTW were investigated by experimeat. The function between average ratio of BCTW and input electron beam was recognized and peak value of the function was the turning point of the critical penetration state in the dynamic process of EBW.

Key words: electron beam welding; beam current through workpiece; characteristic; critical penetrating

Protection of polymer matrix composite material with ceramic coatings GUO Mian-huan, LIU Ai-guo, GAO Jia-shuang, ZHAO Min-hai (State Key Laboratory of Advanced Welding Production Technology, Harbin Institute of Technology, Harbin 150001, China). p13 - 16

Abstract: The bond coating of Al_2O_3 and ZrO_2 light ceramic were sprayed on the carbon fiber reinforced polyimide composite substrate with Al powder sprayed by plasma spaying. And the adhesive strength, thermal cycling resistance, erosion resistance, and heat insulation of the bond coatings were tested. The results showed that, coatings with plasma spray Al bonding layer are better than those with arc spraying Al or Zn bonding layer. Erosion losses of the sample with Al_2O_3 coating are less than 1/3 of that of the PMC substrate. Al_2O_3 and ZrO_2 coatings can provide effective erosion- and thermal-resistance for the PMC substrate, and the thermal-resistance of the ZrO_2 coating is better than that of the Al_2O_3 coating.

Key words: high temperature polymer matrix composite material; ceramic coating; erosion; thermal-resistance coating

Dynamic behavior of plasma in CO_2 laser welding of stainless steel

DUAN Ai-qin[1,2], CHEN Li[1,2], WANG Ya-jun[2], HU Lun-ji[1] (1. Huazhong University of Technology and Science, Wuhan 430074, China; 2. BAMTRI, Key laboratory for high energy density beam processing technology, Beijing 100024, China). p17 - 20

Abstract: Laser induced plasma is an important physical phenomenon in laser deep penetration welding. It has stronger relationsip to stability of process, quality of weld, and efficiency of laser energy. In this paper, two methods were used to study the dynamic behavior of plasma and the influences on stability of welding process. These methods were high-speed camera and optical signal monitoring. The results showed that the dynamic process of plasma can be divided into four steps, (1) material vaporing; (2) plasma increasing; (3) plasma bombing and separating; (4) plasma scattering. The main reason affected welding process stability is the fluctuation of plasma between non-penetration and penetration process.

Key words: Laser welding; laser induced-plasma; high-speed camera; optical signal

Weld residual stress distribution of GH536 superalloy with EBW measuned by Mathar method FU Peng-fei, LIU Fang-jun, FU Gang, MAO Zhi-yong (Key Laboratory of high energy density beam processing technology, Beijing Aeronautical Manufacturing Technology Research Institute, Beijing 100024, China). p21 - 23

Abstract: Electron beam welding is applied to manufacturing many superalloy components of aeroengine, but the researches of weld residual stress were very few for those components. In this paper, weld residual stress of GH536 superalloy components with EBW were measured by Mathar method. Test results showed that residual stress is low in the weld and its distribution accords with the traditional rules. This research can accumulate experiences and properties data for manufacturing aeroengine components with EBW.

Key words: GH536 superalloy; electron beam welding; hole drilling method; residual stress

Real-time monitor system based on virtual instrument technology for laser welding ZHANG Pu, PENG Qi-zhi, KONG Li (Huazhong University of Technology and Science, Wuhan 430074, China). p24 - 26

Abstract: The laser deep penetration welding monitoring system based on the virtual instrument technology was introduced. The component of hardware and the development of software were illuminated. Three signals of ultraviolet light, infrared light and acoustic signal acquired by three special sensors. The raw data were processed dy DSP, multi-sensors data fusion was done by neural network algorithm, and the reliable result of welding quality was oslained. The experimental data proved the system's validity and stability.

Key words: virtual instrument; laser welding; data fusion

Optimization selection of power source frequency in high frequency induction brazing HE Peng, LIU Duo, FENG Ji-cai (National Key Laboratory of Advanced Welding Production Technology, Harbin Institute of Technology, Harbin 150001, China). p27 - 29

Abstract: Appropriate frequency of high frequency power source shoulded be selected to obtain perfect soldered joint during high frequency induction brazing according to the physical performance of joint materials. Numerical selection model for the frequency and its arrange of high frequency induction heating power source was set up by means of numerical analysis. It showed that numerical analysis can be used as an important artifice for design of high frequency power equipment. Compared the analytical results from the numerical model with that of the traditional formula, it showed that the former is more accurate. Because the latter was derived from the plane electromagnetic wave spreading characteristic in electro-conductive inter-media, it was more suitable for the frequency selection of board structure high frequency induction heating. But for frequency selection of pipe-structure or more complex structure high frequency induction heating, the numerical analytical method will be better.

Key words: high frequency induction brazing; power frequency; numerical analysis

Corrosion behavior of weld metal of low-alloy steel HUANG An-guo[1], LI Zhi-yuan[1], YU Sheng-fu[1], ZHOU Long-zao[1], ZHANG Guo-dong[2] (1. School of Materials Science and Engineering, Huazhong University of Science and Technology, Wuhan 430074, China; 2. School of Power and Mechanic, Wuhan Uniersity, Wuhan 430072, China). p30 - 34

Abstract: Two welding heat input were applied to 16Mn and X70 steel by SAW. The corrosion behavior of weld metal was investigated in two kinds of solution, NACE and 3.5% NaCl, respectively. The results show that corrosion tendency of acicular ferrite (AF) in weld is greater than other microstructures, but its corrosion velocity is slowly. The corrosion resistance of weld metal with AF increases with the increasing of ac-